RSC Advances

PAPER

View Article Online
View Journal | View Issue



Cite this: *RSC Adv.*, 2016, **6**, 51642

# Modulation of charge carrier mobility by side-chain engineering of bi(thienylenevinylene)thiophene containing PPE–PPVs†

Rupali R. Jadhav,[ab] Nadia Camaioni,*[c] Kerstin Oppelt,[d] Francesca Tinti,[c] Massimo Gazzano,[c] Valeria Fattori,[c] Prakash P. Wadgaonkar,[b] Silke Rathgeber,[e] Harald Hoppe[fg] and Daniel A. M. Egbe*[a]

Received 11th January 2016
Accepted 19th May 2016

DOI: 10.1039/c6ra00858e

www.rsc.org/advances

Four 2-dimensional conjugated poly(*p*-phenylene-ethynylene)-*alt*-poly(*p*-phenylene-vinylene) polymers containing a lateral bi(thienylenevinylene)thiophene unit (**BTE-PV**s) were synthesised and characterised. The investigated polymers share the same conjugated structure, but differ in the anchoring positions of solubilising linear octyloxy/branched 2-ethylhexyloxy side-chains. UV-vis spectra of the polymers in dilute chloroform solutions and as thin films were studied. X-Ray diffraction patterns as well as the bulk charge transport of polymer films cast from chlorobenzene solutions were also investigated. A dramatic effect of the solubilising side-chains on the charge carrier mobility of **BTE-PV** films was observed, with bulk hole mobility values ranging between $1.3 \times 10^{-5}$ $cm^2$ $V^{-1}$ $s^{-1}$ and $2.2 \times 10^{-2}$ $cm^2$ $V^{-1}$ $s^{-1}$, which is not ascribable to evident structural variations of the polymer films. It is shown that the combination of linear octyloxy and branched 2-ethylhexyloxy side-chains is favorable for the charge transport properties of **BTE-PV**s, compared to the incorporation of only linear or only branched side-chains.

## Introduction

Soluble conjugated polymers have attracted broad academic and industrial interest as innovative semiconducting materials and are promising candidates for cost effective printed electronics owing to their unique combination of solution processability, excellent mechanical properties, and tunability of their electronic properties by structural variations.[1,2] The structural components of conjugated polymers, the backbone as well as side groups, have been appropriately designed in order to meet the specific requirements of a particular electronic application.[3] Organic field-effect transistors (OFETs),[4] photovoltaic cells,[5] and light-emitting diodes (OLEDs)[6] are the key applications of conjugated polymer and for the operation of each of these devices, charge transport constitutes a common and major determining factor. Indeed, the current flowing between source and drain in an OFET is primarily related to charge carrier mobility. High and balanced hole and electron mobilities are required for high performance in solar cells. Balanced charge transport is also required for high efficiency of charge recombination in OLEDs. Given the strong impact of charge carrier mobility on the properties of any electronic device, the knowledge of how to tune the molecular structure of organic conjugated materials to achieve high mobility values is of utmost importance, in addition to the other factors such as molecular packing, disorder, impurities, *etc.*, which also affect charge transport properties of organic films.

It is well known that the nature, size, and position of the solubilising side-chains attached to the conjugated backbone can have a dramatic effect not only on their processability from organic solvents but also on the electronic properties of conjugated polymers.[7–10] Nowadays, two dimensional conjugated polymeric systems comprising the conjugated main chain and conjugated side-chains are intensively studied. Since the first attempt by Li and coworkers,[11] the two-dimensional conjugation concept has emerged as a proven approach for the design of conjugated polymers with improved optoelectronic properties.[12] Considerable research efforts are being made towards decorating highly efficient benzo[1,2-*b*:4,5-*b*′] dithiophene (BDT) based polymers with varied conjugated side

[a]*Linz Institute for Organic Solar Cells, Johannes Kepler University Linz, Altenbergerstr. 69, 4040 Linz, Austria. E-mail: daniel_ayuk_mbi.egbe@jku.at*

[b]*Polymers & Advanced Materials Laboratory, Polymer Science and Engineering Division, CSIR – National Chemical Laboratory, Dr. Homi Bhabha Road, Pune 411008, Maharashtra, India*

[c]*Istituto per la Sintesi Organica e la Fotoreattività, Consiglio Nazionale delle Ricerche, via P. Gobetti 101, I-40129 Bologna, Italy. E-mail: nadia.camaioni@isof.cnr.it*

[d]*Institute of Inorganic Chemistry, Johannes Kepler University Linz, Altenbergerstr. 69, 4040 Linz, Austria*

[e]*Institute for Integrated Natural Sciences, University of Koblenz-Landau, Universitätsstr.1, 56070 Koblenz, Germany*

[f]*Institute of Physics, Ilmenau University of Technology, Weimarer-Str. 32, 98693 Ilmenau, Germany*

[g]*Institute of Organic Chemistry and Macromolecular Chemistry, Friedrich Schiller University, Humboldtstr. 10, 07743, Jena, Germany*

† Electronic supplementary information (ESI) available. See DOI: 10.1039/c6ra00858e

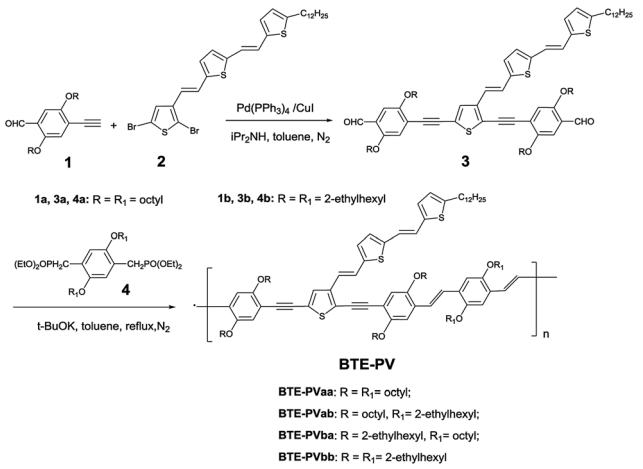


Scheme 1 Synthesis of monomers (**3a**, **3b**) and of conjugated polymers **BTE-PV**s.

groups to achieve higher power conversion efficiencies.[13–23] Recently, Hou *et al.* have also shown the modulating effect of the two-dimensional structure on reaching higher mobility in case of 2-alkylthienyl substituted benzo[1,2-*b*:4,5-*b*′]dithiophene (BDT) based polymer, namely PBDT-TS1.[24]

Previously, we have systematically studied the effect of various alkoxy side-chains of different lengths and nature (linear or branched) on anthracene-containing poly(*p*-phenylene-ethynylene)-*alt*-poly(*p*-phenylene-vinylene) (PPE–PPV) copolymers[7,25,26] and the strong dependence of the structural, optical, and electrical properties of the investigated polymer films on the lateral side-chains has been demonstrated. In this contribution, polymers with a two-dimensional conjugated system are considered. PPE–PPVs incorporating a bithienylene-vinylene thiophene group as a conjugated side-group on the PPE unit (**BTE-PV**s) and bearing octyloxy or 2-ethylhexyloxy side-chains on the BTE and PV parts were synthesised (Scheme 1), in order to investigate how their electronic properties can be modulated by simultaneous incorporation of conjugated as well as alkoxy side-chains. In these polymers, the bithienylene-vinylene thiophene group extends the conjugation in the lateral direction and an improved degree of the electronic interactions between the polymer chains is expected in the solid state, compared to a conventional linear conjugated structure.[12] Thus, the conjugated lateral group together with the alkoxy solubilising chains is expected to affect charge carrier mobility of the polymeric films under investigation. Indeed, the **BTE-PV** polymer containing the branched 2-ethylhexyloxy chain in the BTE unit and the linear octyloxy chain in the PV unit exhibited a remarkable hole mobility of $2.2 \times 10^{-2}$ $cm^2$ $V^{-1}$ $s^{-1}$ at a moderate applied electric field of $8 \times 10^4$ V $cm^{-1}$.

# Experimental

## Materials

The various starting materials were purchased from commercial suppliers (Sigma, Aldrich, and Fluka) and were used without further purification, unless specified. Solvents were dried and distilled according to standard procedures and stored under argon. If not otherwise specified solvents or solutions were degassed for 1 h with nitrogen or argon prior to use.

4-Ethynyl-2,5-dioctyloxybenzaldehyde (**1a**),[27] 4-ethynyl-2,5-di(2-ethyl)hexyloxy-benzaldehyde (**1b**),[27] 2,5-dibromo-3-(1-*E*)-2-(5-((2-(5-dodecylthiophen-2-yl)vinyl)thiophen-2-yl)vinyl)thiophene (**2**),[11] 2,5-dioctyloxy-*p*-xylylenebis(diethylphosphonate) (**4a**) and 2,5-di(2-ethyl)hexyloxy-*p*-xylylenebis(diethylphosphonate) (**4b**)[28] were synthesized according to the literature procedures. The synthetic routes of monomers and polymers are shown in Scheme 1.

## Synthesis of monomers and polymers

**2,5-Bis{[(2,5-dioctyloxy-4-formyl)phenyl]ethynyl}-3-(2-{5-[2-(5-dodecyl)thiophenyl]vinyl}thiophenyl)vinyl-thiophene (3a).** 4-Ethynyl-2,5-dioctyloxybenzaldehyde (**1a**) (0.80 g, 1.28 mmol) and 2,5 dibromo-3-(1-*E*)-2-(5-((2-(5-dodecylthiophen-2-yl)vinyl) thiophen-2-yl)vinyl)thiophene (**2**) (1.55 g, 4.01 mmol) were dissolved in a mixture of 50 mL toluene and 20 mL diisopropylamine and the reaction mixture was degassed for 1 h in an argon atmosphere. The catalysts $Pd(PPh_3)_4$ (166.4 mg, 0.14 mmol) and CuI (28 mg, 0.14 mmol) were then added into the solution and the mixture was heated at 80 °C for 24 h in argon atmosphere. After cooling to room temperature, the precipitated diisopropylammonium bromide was filtered off and the solvent was distilled off under vacuum. The residue was purified by column chromatography on silica gel with toluene as an eluent to afford pure **3a** as a dark-red viscous liquid ($R_f = 0.8$, 0.87 g, 56%). $^1$H NMR ($CDCl_3$, 500 MHz): $\delta$/ppm 0.85–0.92 (m, 15H, $-CH_3$), 1.18–1.29 (m, 48H, $-CH_2-$), 1.44–1.53 (m, 10H, $-C\underline{H}_2-CH_3$), 1.64–1.69 (m, 2H, $-CH_2-C\underline{H}_2-(CH_2)_9CH_3$ of dodecyl chain), 1.82–1.90 (m, 8H, $-O-CH_2-C\underline{H}_2-(CH_2)_5CH_3$), 2.72, 2.80 (two triplets, 2H, $-C\underline{H}_2-CH_2-(CH_2)_9CH_3$, first methylene of dodecyl chain which is directly attached to thiophene ring), 4.07 (t, 8H, $-O-CH_2-$), 6.59–7.26 (multiple peaks, 9H, vinylic and thiophene protons) 7.33–7.49 (multiple peaks, 4H, $C_{phenyl}$–H), 10.47 (s, 2H, –CHO).

**2,5-Bis({[2,5-di(2-ethyl)hexyloxy-4-formyl]phenyl}ethynyl)-3-(2-{5-[2-(5-dodecyl)thiophenyl]vinyl}thiophenyl)vinyl-thiophene (3b).** The dialdehyde **3b** was synthesised using the same procedure as that given for **3a** but with **1a** (0.90 g, 2.32 mmol) and **2** (0.73 g, 1.16 mmol) as starting materials and using $Pd(PPh_3)_4$ (53.8 mg, 0.046 mmol) and CuI (8.80 mg, 0.046 mmol) as catalysts. Pure **3b** was obtained as a dark red viscous liquid ($R_f = 0.8$, 0.90 g, 63%). $^1$H NMR ($CDCl_3$, 500 MHz): $\delta$/ppm 0.78–0.94 (m, 27H, $-CH_3$), 1.25–1.39 (m, 40H, $-CH_2-$), 1.49–1.56 (m, 10H, $-C\underline{H}_2-CH_3$), 1.66–1.70 (m, 2H, $-CH_2-C\underline{H}_2-(CH_2)_9CH_3$ of dodecyl chain), 1.76–1.85 (m, 4H, $-O-CH_2-C\underline{H}(CH_2CH_3)-(CH_2)_3CH_3$), 2.79 (t, 2H, $-C\underline{H}_2-CH_2-(CH_2)_9CH_3$, first methylene of dodecyl chain which is directly attached to thiophene ring), 3.97 (d, 8H, $-O-C\underline{H}_2-CH(CH_2CH_3)(CH_2)_3CH_3$), 6.56–7.26 (multiple peaks, 9H, vinylic and thiophene protons), 7.30–7.49 (multiple peaks, 4H, $C_{phenyl}$–H), 10.47 (s, 2H, –CHO).

**Polymer BTE-PV*ab*.** 2,5-Bis{[(2,5-dioctyloxy-4-formyl)phenyl]ethynyl}-3-(2-{5-[2-(5-dodecyl)thiophenyl]vinyl}thiophenyl)vinyl-thiophene (**3a**) (0.56 g, 0.45 mmol) and 2,5-di(2-ethyl)hexyloxy-*p*-xylylenebis(diethylphosphonate) (**4b**) (0.29 g, 0.45 mmol) were dissolved in 50 mL of dried toluene by vigorous stirring under

argon atmosphere and then allowed to reflux. Potassium-*tert*-butoxide (0.41 g, 3.62 mmol) was added into the refluxing solution, which made the reaction to become successively darker and viscous. The reaction mixture was then heated at reflux for 3 h. After this, benzaldehyde (1 mL) was added for end-capping of the polymer. The reaction was stopped after half an hour after addition of benzaldehyde. It was allowed to cool down and quenched with aqueous HCl. The organic phase was separated and extracted several times with distilled water until the aqueous phase becomes neutral (pH = 6–7). The organic layer was dried in Dean–Stark apparatus. The resulting toluene solution was filtered, concentrated and precipitated in cold methanol to get dark-brown coloured polymer. The polymer was then purified by Soxhlet extraction with methanol/diethylether mixture (1 : 1 v/v) for 3 h. The obtained sticky polymer was again dissolved in a small amount of toluene, precipitated in methanol and dried under vacuum to obtain dark-red colored polymer (0.49 g, 69%). $^1$H NMR ($CDCl_3$, 500 MHz): $\delta$/ppm 0.8–0.95 (m, 27H, –$CH_3$), 1.17–1.34 (m, 60H, –$CH_2$–), 1.45–1.56 (m, 14H, –C$\underline{H}_2$–$CH_3$ of alkyl chains), 1.66–1.70 (m, 2H, –$CH_2$–C$\underline{H}_2$–$(CH_2)_9CH_3$ of dodecyl chain), 1.76–1.94 (m, 10H, –O–$CH_2$–C$\underline{H}_2$–$(CH_2)_5CH_3$ in octyl and –O–$CH_2$–C$\underline{H}$($CH_2CH_3$)$(CH_2)_3CH_3$ in 2-ethylhexyl side-chain), 2.79 (t, 2H, –C$\underline{H}_2$–$CH_2$–$(CH_2)_9CH_3$, first methylene of dodecyl chain which is directly attached to thiophene ring), 3.88–4.17 (m, 12H, –O–$CH_2$–), 6.61–7.60 (multiple peaks, 19H, $C_{phenyl}$–H, thiophene protons, vinylic protons in both the side-chain and the polymer backbone). GPC (PS standards): $M_w$ = 26 640 g mol$^{-1}$, $M_n$ = 11 100 g mol$^{-1}$, PDI = 2.4.

**Polymer BTE-PV*aa*.** Polymer **BTE-PV*aa*** was synthesised using the same procedure as that given for **BTE-PV*ab*** but with **3a** (0.70 g, 0.57 mmol), **4a** (0.36 g, 0.57 mmol) as starting materials and potassium-*tert*-butoxide (0.48 g, 4.28 mmol) as a base. **BTE-PV*aa*** was collected as a dark reddish brown solid. (0.54 g, 0.34 mmol, 61%). $^1$H NMR ($CDCl_3$, 500 MHz): $\delta$/ppm 0.86–0.90 (m, 21H, –$CH_3$), 1.24–1.34 (m, 64H, –$CH_2$–), 1.54–1.58 (m, 14H, –C$\underline{H}_2$–$CH_3$), 1.66–1.69 (m, 2H, –$CH_2$–C$\underline{H}_2$–$(CH_2)_9CH_3$ of dodecyl chain), 1.83–1.93 (m, 12H, –O–$CH_2$–C$\underline{H}_2$–$(CH_2)_5CH_3$), 2.71–2.80 (t, 2H, –C$\underline{H}_2$–$CH_2$–$(CH_2)_9CH_3$, first methylene of dodecyl chain which is directly attached to thiophene ring), 3.96–4.17 (t, 12H, –O–$CH_2$), 6.61–7.65 (multiple peaks, 19H, $C_{phenyl}$–H, thiophene protons, vinylic protons in both the side-chain and the polymer backbone). GPC (PS standards): $M_w$ = 47 800 g mol$^{-1}$, $M_n$ = 26 700 g mol$^{-1}$, PDI = 1.8.

**Polymer BTE-PV*bb*.** Polymer **BTE-PV*bb*** was synthesised using the same procedure as that given for **BTE-PV*ab*** but with **3b** (0.30 g, 0.25 mmol), **4b** (0.16 g, 0.25 mmol) as starting materials and potassium-*tert*-butoxide (0.11 g, 0.10 mmol) as a base. **BTE-PV*bb*** was collected as a dark brown solid (0.19 g, 0.12 mmol, 49%). $^1$H NMR ($CDCl_3$, 500 MHz): $\delta$/ppm 0.75–1.0 (m, 39H, –$CH_3$), 1.21–1.41 (m, 52H, –$CH_2$–), 1.43–1.51 (m, 14H, –C$\underline{H}_2$–$CH_3$), 1.66–1.69 (m, 2H, –$CH_2$–C$\underline{H}_2$–$(CH_2)_9CH_3$ of dodecyl chain), 1.77–1.91 (m, 6H, –O–$CH_2$–C$\underline{H}$($CH_2CH_3$)$(CH_2)_3CH_3$), 2.79 (t, 2H, –$CH_2$– directly attached to thiophene ring in side-chain), 3.77–4.11 (m, 12H, –O–$CH_2$), 6.61–7.65 (multiple peaks, 19H, $C_{phenyl}$–H, thiophene protons, vinylic protons in both the side-chain and the polymer backbone). GPC (PS standards): $M_w$ = 25 200 g mol$^{-1}$, $M_n$ = 10 500 g mol$^{-1}$, PDI = 2.4.

**Polymer BTE-PV*ba*.** Polymer **BTE-PV*ba*** was synthesised using the same procedure as that given for **BTE-PV*ab*** but with **3b** (0.59 g, 0.48 mmol), **4a** (0.30 g, 0.48 mmol) as starting materials and potassium-*tert*-butoxide (0.42 g, 3.75 mmol) as a base. **BTE-PV*ba*** was collected as a dark reddish brown solid (0.28 g, 0.18 mmol, 40%). $^1$H NMR ($CDCl_3$, 500 MHz): $\delta$/ppm 0.81–0.96 (m, 33H, –$CH_3$), 1.26–1.65 (m, 72H, –$CH_2$–), 1.78–1.90 (m, 8H, –O–$CH_2$–C$\underline{H}_2$–$(CH_2)_5CH_3$ in octyl and –O–$CH_2$–C$\underline{H}$($CH_2CH_3$)$(CH_2)_3CH_3$ in 2-ethylhexyl side-chain), 2.79 (t, 2H, –C$\underline{H}_2$–$CH_2$–$(CH_2)_9CH_3$, first methylene of dodecyl chain which is directly attached to thiophene ring), 3.64–4.18 (m, 12H, –O–$CH_2$), 6.64–7.65 (multiple peaks, 19H, $C_{phenyl}$–H, thiophene protons, vinylic protons in both the side-chain and the polymer backbone). GPC (PS standards): $M_w$ = 12 390 g mol$^{-1}$, $M_n$ = 5900 g mol$^{-1}$, PDI = 2.1.

## Characterisation

All compounds were characterized by nuclear magnetic resonance spectra (NMR) recorded on a Bruker AV 500 spectrometer in $CDCl_3$ at room temperature. Molecular weights and distributions of the copolymers were estimated by the gel permeation chromatography (GPC) method, THF as the eluent and polystyrene as the standard. The absorption and emission spectra were determined by Perkin Elmer Lambda 950 spectrophotometer and Spex Fluorolog fluorometer respectively.

## Photophysical characterization

Dilute solutions of the different polymers in chloroform ($5 \times 10^{-7}$ mol L$^{-1}$ per repeating unit) and thin films spin-cast from chlorobenzene solutions (8–14 g L$^{-1}$) on polished quartz substrates were prepared for the photophysical characterization. After the deposition, the films were solvent–vapor annealed (chlorobenzene) overnight. Smooth and uniform films with a thickness of about 120 nm were used for the photophysical characterization. Quantum yields in solution were obtained by using an air-equilibrated $Ru(bipy)_3Cl_2$ solution as the reference ($\Phi$ = 0.28).[29] The absorption and emission spectra were determined by using a Perkin Elmer Lambda 950 spectrophotometer and a Spex Fluorolog fluorometer, respectively. The same Spex Fluorolog fluorometer equipped with a custom-made integrating sphere system was employed for absolute measurements of the film emission quantum yields. The estimated error for the quantum yield data is 20%. Photoluminescence lifetimes were determined with an IBH 5000F time-correlated single-photon counting device, by using a pulsed NanoLED excitation source at 465 nm. The analysis of the luminescence decay profiles was accomplished with the Decay Analysis Software DAS6 provided by the manufacturer. The estimated error on the lifetime is 10%. All measurements were performed at room temperature in ambient atmosphere in a single experimental session for each group of measurements in order to get rid of experimental errors which could affect comparison of the different polymer spectra, lifetimes and quantum yields.

## Time of flight (TOF)

Polymer films for time of flight experiments were drop-cast onto aluminium-coated glass substrates from chlorobenzene solutions

 

(concentrations ranging between 18 and 33 g $L^{-1}$ for the four polymers). After the deposition, the films were solvent–vapour annealed (chlorobenzene) overnight to obtain uniform films. The device structure was completed with a vacuum-evaporated semi-transparent aluminium electrode (18 nm thick). The device area was 0.25 $cm^2$ and the film thicknesses were 4.7, 4.6, 10, and 11.4 μm for **BTE-PV*aa***, **BTE-PV*ab***, **BTE-PV*ba***, and **BTE-PV*bb***, respectively. A nitrogen laser ($\lambda = 337$ nm) with a pulse duration of 6–7 ns was used to photogenerate charge carriers in TOF experiments. The penetration depth of light was 400 nm for all the investigated films, that is at least one order of magnitude lower than film thickness. A variable DC potential was applied to the samples and in order to ensure a uniform electric field inside the device, the total photo-generated charge was kept less than $0.1CV$ (where $C$ is the sample capacitance and $V$ the applied potential) by attenuating the laser beam intensity with quartz neutral filters. The photocurrent was monitored across a variable load resistance by using a Tektronix TDS620A digital oscilloscope. TOF measurements were performed at room temperature and under dynamic vacuum ($10^{-5}$ mbar).

### X-ray diffraction (XRD)

Polymer films for XRD investigations were drop-cast from the same chlorobenzene solutions which were used for the preparation of TOF samples. Mineral quartz 'zero background' was used as the substrate (The Gem Dugout, State College, PA-USA), in order to strongly minimize its contribution to the total scattering. After deposition, the films were solvent–vapour annealed in chlorobenzene overnight. XRD analysis was carried out by means of a PANalytical X'Pert diffractometer equipped with a copper anode ($\lambda_{mean} = 0.15418$ nm) and a fast X'Celerator detector, with a step of 0.05° ($2\theta$) and counting time of 120 s per step. The films were directly investigated in reflection geometry.

## Results and discussion

### Synthesis and characterization

Four side-chain conjugated polymers namely **BTE-PV*aa***, **BTE-PV*ab***, **BTE-PV*bb***, **BTE-PV*ba*** were synthesized. The requisite dialdehyde monomers, 2,5-bis{[(2,5-dialkoxy-4-formyl)phenyl] ethynyl}-3-(2-{5-[2-(5-dodecyl)thiophenyl]vinyl}thiophenyl)vinyl-thiophene (**3a**/**3b**) were synthesised by Pd-catalysed Sonogashira cross-coupling reaction between 4-ethynyl-2,5-dialkoxy-benzaldehyde (**1a**/**1b**) and 2,5-dibromo-3-(1-*E*)-2-(5-((2-(5-dodecylthiophen-2-yl)vinyl)thiophen-2-yl)vinyl)thiophene (**2**). The polymers were synthesised by Horner–Wadsworth–Emmons olefination reaction of the dialdehydes (**3a**, **3b**) with bisphosphonate esters (**4a**, **4b**) in the presence of potassium *tert*-butoxide, based on well-established protocols.[7]

The four polymers have an identical backbone but differ in the solubilising side-chains (linear or branched/a or b) on the BTE and PV parts on the polymer. Solely linear (**BTE-PV*aa***), solely branched (**BTE-PV*bb***) and mixed linear and branched (**BTE-PV*ab***, **BTE-PV*ba***) side-chains were appended to the polymer backbone. The polymers were obtained in yields between 40% and 69% after extraction with methanol/diethylether mixture (1 : 1, v/v). The number-average molecular weights of **BTE-PV*aa***, **BTE-PV*ab***, **BTE-PV*bb***, **BTE-PV*ba*** are 26.7, 11.1, 10.5 and 5.9 kg $mol^{-1}$, with the corresponding dispersity to be 1.8, 2.4, 2.4, and 2.1 respectively. They were soluble in common organic solvents such as chloroform, dichloromethane, tetrahydrofuran, toluene and chlorobenzene. The chemical structures of the polymers were confirmed by $^1$H NMR and $^{13}$C-NMR spectroscopy. Fig. S1 and S2† depict representative $^1$H-NMR spectrum of dialdehyde **3a** and polymer **BTE-PV*ab*** respectively.

### Photophysical investigations

Fig. 1a displays the normalized absorption and emission spectra in dilute chloroform solutions. The spectra of the polymers in dilute solution show absorption maxima between 445–450 nm and emission peaks between 540–544 nm. Quantum yields and lifetimes of the four polymers are also very similar (Table 1). This indicates that the polymer backbone organization and conjugation in dilute solution are less affected by the nature of the solubilising chains. The normalized absorption and emission spectra of thin films are depicted in Fig. 1b, which shows that the different solubilizing side-chains slightly affect the polymer aggregation in the films.[30] Thin-film absorption spectra of polymers **BTE-PV*bb*** and **BTE-PV*ba*** are

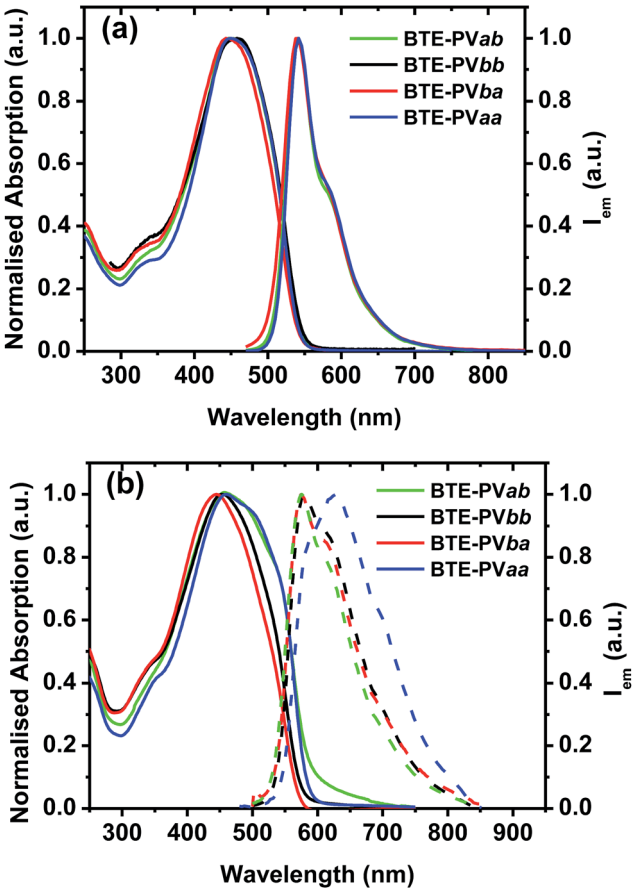


Fig. 1 Normalized absorption (solid) and emission (dash) spectra of the polymers (a) in dilute chloroform solutions and (b) of the polymer films.

Table 1 Photophysical data in dilute chloroform solution and thin film

| | Dilute solution | | | | Thin film | | | |
|---|---|---|---|---|---|---|---|---|
| | $\lambda_{abs}$ (nm) | $\lambda_{em}$ (nm) | $\Phi_\phi$ | $\tau$ (ns) | $\lambda_{abs}$ (nm) | $\lambda_{em}$ (nm) | $\Phi_\phi$ | $\tau^a$ (ns) |
| **BTE-PV*ab*** | 450 | 542 | 0.28 | 0.9 | 460 (540 sh) | 580 (610 sh) | 0.019 | 0.2 |
| **BTE-PV*bb*** | 450 | 544 | 0.24 | 0.9 | 460 | 575 (610 sh) | 0.010 | ≤0.2 |
| **BTE-PV*ba*** | 450 | 540 | 0.27 | 0.9 | 445 | 575 (610 sh) | 0.015 | ≤0.2 |
| **BTE-PV*aa*** | 450 | 542 | 0.26 | 0.9 | 460 (540 sh) | 630 (585 sh) | 0.012 | ≤0.2 |

[a] 200 ps is the shortest time that can be resolved with the used experimental system.

slightly red shifted and broadened with respect to the solution ones, as a consequence of polymer–polymer interactions. For **BTE-PV*ab*** and **BTE-PV*aa*** a broadening of the absorption band with a shoulder peak at around 540 nm points out to a more effective interaction between polymer backbones. In particular, for **BTE-PV*aa*** a strong optical coupling of the polymer chains is effective, as demonstrated by the large red shift of the emission band. Evidently, the linear octyloxy side-chains help the solid state organization of polymer backbones. The quantum yields are similar for all polymers in thin films (Table 1) and are about 20 times lower than the solution values, while the luminescence lifetimes drop below 200 ps (the luminescence decay curves are reported in Fig. S3†). Both effects are due to a faster non-radiative decay of the excited states in the films.

## Charge carrier mobility

The drift mobility of charge carriers was studied as a function of the applied electric field ($E$) by using differential small-signal time of flight (TOF).[31] The TOF experiments were performed on sandwich-type devices with the structure glass/Al/polymer/Al, with the top aluminium layer being semi-transparent for sample irradiation. For a better comparison of the charge transport properties of the investigated polymers, the same conditions were used for the film deposition. The sign of charge carriers generating the TOF photocurrent signals was selected by appropriately biasing the illuminated electrode (positively biased for holes, negatively biased for electrons).

This class of conjugated polymers show an ambipolar behavior.[32] Typical photocurrent transients, for holes and electrons, are displayed in Fig. S4† in a double-logarithmic representation and for a comparable applied electric field of about $8 \times 10^4$ V cm$^{-1}$. Though the dispersion of photocurrent signals, an inflection point was visible in the double-logarithmic plots, from which the transit time ($t_{tr}$) of charge carriers can be evaluated.[33] In the case of **BTE-PV*ba***, it was not possible to detect the photocurrent signal for negative carriers, presumably because of very short transit times of electrons for this polymer.

The values of charge carrier mobility ($\mu$) were calculated as a function of the applied electric field $E$ through the well-known expression $\mu = d/t_{tr}E$ where $d$ is the thickness of the polymer layer, and with the transit times extracted from the TOF signals by using the same method in all cases, that is from the inflection point observed in the double-logarithmic representation. The mobility data are reported in Fig. 2, which clearly shows the dramatic effect of the lateral solubilising chains on charge carrier mobility, with $\mu$ varying by orders of magnitude for the polymers under consideration. For a better comparison, the mobility values at a comparable electric field of about $8 \times 10^4$ V cm$^{-1}$ are collected in Table 2. The drift mobility of positive carriers ($\mu_h$) was found to vary from $1.3 \times 10^{-5}$ cm$^2$ V$^{-1}$ s$^{-1}$ for **BTE-PV*aa*** to $2.2 \times 10^{-2}$ cm$^2$ V$^{-1}$ s$^{-1}$ for **BTE-PV*ba*** at $E$ of around $8 \times 10^4$ V cm$^{-1}$. Similarly, the drift mobility of electrons ($\mu_e$) showed a great variation by changing the solubilising side-chains.

## X-ray diffraction

Transport of charge carriers is highly affected by the organization of polymer chains in the solid state.[34,35] Thus, X-ray

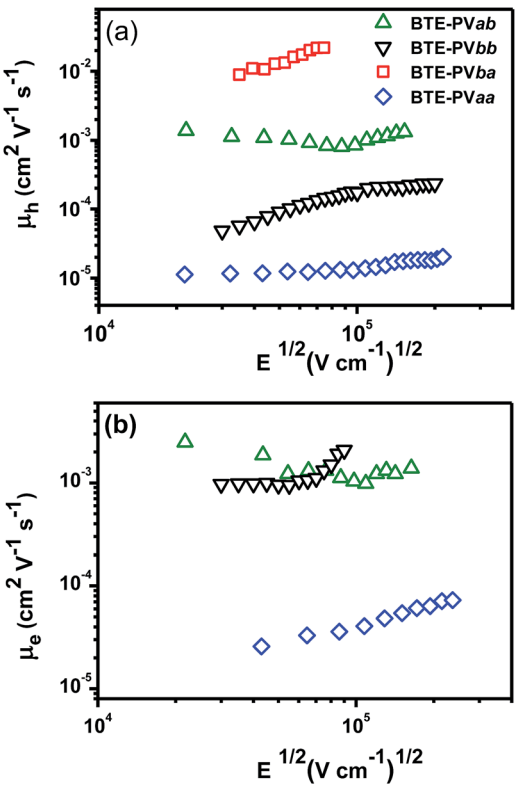


Fig. 2 Hole mobility (a) and electron mobility (b) as a function of the square root of the electric field for: BTE-PV*aa* (blue diamonds); BTE-PV*ab* (green triangles); BTE-PV*ba* (red squares); BTE-PV*bb* (inverted triangles).

 

Table 2 Hole and electron mobility for an electric field of around $8 \times 10^4$ V cm$^{-1}$

| Polymer | $\mu_h$ (cm$^2$ V$^{-1}$ s$^{-1}$) | $\mu_e$ (cm$^2$ V$^{-1}$ s$^{-1}$) |
|---|---|---|
| **BTE-PV*ab*** | $8.4 \times 10^{-4}$ | $1.3 \times 10^{-3}$ |
| **BTE-PV*bb*** | $1.4 \times 10^{-4}$ | $1.3 \times 10^{-3}$ |
| **BTE-PV*ba*** | $2.2 \times 10^{-2}$ | n.a. |
| **BTE-PV*aa*** | $1.3 \times 10^{-5}$ | $3.6 \times 10^{-5}$ |

diffraction was performed on polymer films prepared under the same conditions used for TOF experiments, in order to evaluate the effect of possible structural variations induced by the different solubilising side-chains. XRD patterns of the four samples are compared in Fig. 3. All the samples show the typical pattern of a disordered solid, nevertheless a few differences can be appreciated. In more detail, the samples **BTE-PV*aa*** and **BTE-PV*ab***, richer in the linear octyloxy chains, show an asymmetric amorphous halo with intensity maximum at 2 theta of 22.7° (corresponding to 0.39 nm) while for **BTE-PV*bb*** and **BTE-PV*ba***, richer in the branched substituents, the symmetric halo is centred at about 20.8° (0.42 nm). It seems that the pattern shape of **BTE-PV*aa*** and **BTE-PV*ab*** samples is affected by the tentative packing of the methylene units: indeed the position of the two main peaks of polyethylene packing is 21.6° and 24.1°. The sample **BTE-PV*aa*** shows an additional very low intensity reflection at 3.91° (2.2 nm) which suggests an initial stage of ordering in the sample with all linear substituents and seems to recall the broadening of the absorption spectrum observed for **BTE-PV*aa*** thin-film (Fig. 1b). In the overall the XRD patterns indicate the complete amorphous features of all investigated films prepared under the same conditions used for TOF experiments, suggesting that the great variation observed for the drift mobility of charge carriers cannot be attributed to a significantly different organization of polymer chains in the solid state.

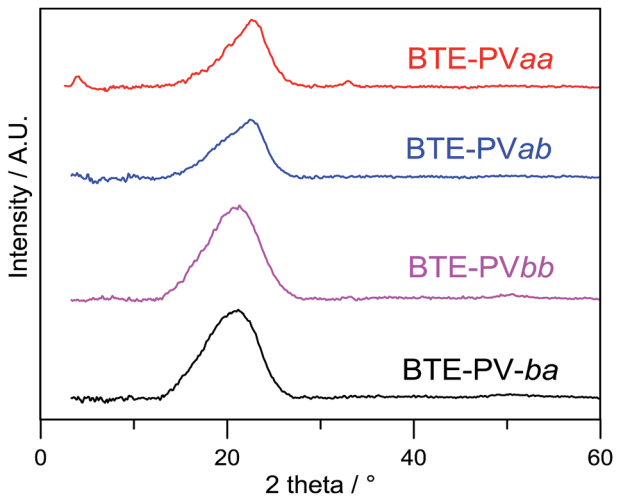


Fig. 3 XRD patterns of polymer films drop-cast onto zero-background quartz substrate.

The inspection of mobility data suggests that the combination of linear and branched substituents (**BTE-PV*ab*** and **BTE-PV*ba***) is favourable for charge transport properties of the investigated polymers, compared to the incorporation of only linear (**BTE-PV*aa***) or only branched side-chains (**BTE-PV*bb***), as already reported for anthracene-containing poly(*p*-arylene-ethynylene)-*alt*-poly(*p*-arylene-vinylene) copolymers (**AnE-PV**s), carrying linear and branched alkoxy side-chains as well as combinations thereof. Indeed it has been observed that the partial substitution of branched 2-ethylhexyloxy side-chains leads to less organized **AnE-PV**s, compared to all-linear substituted ones. However, unlike the increased disorder, charge carrier mobility of partially substituted **AnE-PV**s was not negatively affected, due to a face-on alignment promoted by the branched side-chains. Differently from **AnE-PV**s,[36] the **BTE-PV**s films here investigated have a common amorphous feature, however the wide range of obtained mobility values could suggest that the mixed linear-branched approach could promote favorable intermolecular interactions for charge transport. The drift mobility of holes in **BTE-PV*ba***, richer in branched substituents compared with **BTE-PV*ab*** also bearing a combination of linear and branched side chains, reaches values of $10^{-2}$ cm$^2$ V$^{-1}$ s$^{-1}$ for a moderate applied electric field (<$10^5$ V$^{-1}$ cm$^{-1}$), which is certainly remarkable for the bulk mobility of amorphous polymer films. The short range ordering is reported to facilitate intermolecular charge transport as demonstrated by Salleo *et al.*[37] Given the low molecular weight of **BTE-PV*ba*** (5.9 kg mol$^{-1}$) in the series, one cannot rule out the possibility of having short chain extended molecules for **BTE-PV*ba***. The presence of short chain extended molecules have been reported to enhance aggregation and thus the charge carrier mobility in the case of poly(3-hexylthiophene).[38] However, this is unlikely in the present case because **BTE-PV*ba*** does not show aggregation in the UV-vis spectrum of the film.

## Conclusions

The four side chain conjugated polymers, differing for the anchoring positions of linear octyloxy and branched 2-ethylhexyloxy solubilising chains on the BTE and PPV units, were synthesised and characterised. The polymers exhibited very different charge transport properties, investigated by TOF technique. The bulk hole mobility at a field of about $8 \times 10^4$ V cm$^{-1}$ ranged from $1.3 \times 10^{-5}$ cm$^2$ V$^{-1}$ s$^{-1}$ for **BTE-PV*aa***, substituted with solely linear chains, to the outstanding value of $2.2 \times 10^{-2}$ cm$^2$ V$^{-1}$ s$^{-1}$ for **BTE-PV*ba***, with branched and linear solubilising chains. The XRD investigation, carried out on thick samples (microns) prepared under the same conditions used for the TOF experiments did not reveal meaningful differences in the structure of the polymer films. In the overall, the XRD patterns indicated a complete amorphous feature. Although the absorption spectra of the thin films suggested a moderate organization for the polymers containing linear octyloxy chains (**BTE-PV*ab*** and **BTE-PV*aa***), no obvious evidence of long-range ordering appeared in the XRD spectra of thick films. Given the similarity of the structural properties of the polymer films, the remarkable difference of mobility values, spanning over

three orders of magnitude, could be mainly attributed to the chemical structure of the polymers. Thus, the combination of linear and branched chains on the BTE and PPV units was found to be favorable for the charge transport properties of the investigated polymers, compared to the incorporation of only linear or branched side-chains, similar to the behaviour already reported for **AnE-PV** copolymers.

## Acknowledgements

R. R. Jadhav, D. A. M. Egbe, H. Hoppe and S. Rathgeber acknowledge the financial support of the Deutsche Forschungsgemeinschaft in the framework of the priority program SPP1355. D. A. M. Egbe also acknowledges the financial support of FWF through project No. I 1703-N20. We thank Prof. Niyazi S. Sariciftci for facilities provided at LIOS, JKU, Linz, Austria and Dr Eckhard Birckner of the University of Jena, Germany, for photophysical measurements.

## References

1 D. Gamota, P. Brazis, K. Kalyanasundaram and J. Zhang, *Printed Organic and Molecular Electronic*, Springer, Kluwer Academic, Norwell, 2004.
2 A. J. Heeger, *Chem. Soc. Rev.*, 2010, **39**, 2354–2371.
3 X. Guo, M. Baumgarten and K. Muellen, *Prog. Polym. Sci.*, 2013, **38**, 1832–1908.
4 C. Wang, H. Dong, W. Hu, Y. Liu and D. Zhu, *Chem. Rev.*, 2012, **112**, 2208–2267.
5 G. Li, R. Zhu and Y. Yang, *Nat. Photonics*, 2012, **6**, 153–161.
6 J. Bolink, E. Coronado, D. Repetto, M. Sessolo, M. Barea, J. Bisquert, G. Garcia-Belmonte, J. Prochazka and L. Kavan, *Adv. Funct. Mater.*, 2008, **18**, 145–150.
7 D. A. M. Egbe, B. Carbonnier, E. Birckner and U.-W. Grummt, *Prog. Polym. Sci.*, 2009, **34**, 1023–1067.
8 S. Lee, H. Cho, K. Cho and Y. Park, *J. Phys. Chem. C*, 2013, **117**, 11764–11769.
9 T. Lei, J.-Y. Wang and J. Pei, *Chem. Mater.*, 2014, **26**, 594–603.
10 J. Mei and Z. Bao, *Chem. Mater.*, 2014, **26**, 604–615.
11 J. Hou, Z. Tan, Y. Yan, Y. He, C. Yang and Y. Li, *J. Am. Chem. Soc.*, 2006, **128**, 4911–4916.
12 Y. Li, *Acc. Chem. Res.*, 2012, **45**, 723–733.
13 F. Huang, K. Chen, H. Yip, S. Hau, O. Acton, Y. Zhang, J. Luo and A. K. Y. Jen, *J. Am. Chem. Soc.*, 2009, **131**, 13886–13887.
14 Q. Peng, X. Liu, D. Su, G. Fu, J. Xu and L. Dai, *Adv. Mater.*, 2011, **23**, 4554–4558.
15 E. Zhou, J. Cong, K. Hashimoto and K. Tajima, *Energy Environ. Sci.*, 2012, **5**, 9756–9759.
16 R. Kularatne, P. Sista, H. Nguyen, M. Bhatt, M. Biewer and M. Stefan, *Macromolecules*, 2012, **45**, 7855–7862.
17 S. Liao, H.-J. Jhuo, Y. Cheng and S. Chen, *Adv. Mater.*, 2013, **25**, 4766–4771.
18 L. Ye, S. Zhang, L. Huo, M. Zhang and J. Hou, *Acc. Chem. Res.*, 2014, **47**, 1595–1603.
19 J. Lee, J.-H. Kim, B. Moon, H. G. Kim, M. Kim, J. Shin, H. Hwang and K. Cho, *Macromolecules*, 2015, **48**, 1723–1735.
20 G. Li, Z. Lu, C. Li and Z. Bo, *Polym. Chem.*, 2015, **6**, 1613–1618.
21 M. Wang, D. Ma, K. Shi, S. Shi, S. Chen, C. Huang, Z. Qiao, Z. G. Zhang, Y. Li, X. Li and H. Wang, *J. Mater. Chem. A*, 2015, **3**, 2802–2814.
22 J. Yuan and W. Ma, *J. Mater. Chem. A*, 2015, **3**, 7077–7085.
23 H. Wu, B. Zhao, W. Wang, Z. Guo, W. Wei, Z. An, C. Gao, H. Chen, B. Xiao, Y. Xie, H. Wu and Y. Cao, *J. Mater. Chem. A*, 2015, **3**, 18115–18126.
24 L. Ye, S. Zhang, W. Zhao, H. Yao and J. Hou, *Chem. Mater.*, 2014, **26**, 3603–3605.
25 D. A. M. Egbe, S. Türk, S. Rathgeber, F. Kuehnlenz, R. Jadhav, A. Wild, E. Birckner, G. Adam, A. Pivrikas, V. Cimrova, G. Knör, N. S. Sariciftci and H. Hoppe, *Macromolecules*, 2010, **43**, 1261–1269.
26 F. Tinti, F. Sabir, M. Gazzano, S. Righi, Ö. Usluer, C. Ulbricht, T. Yohannes, D. A. M. Egbe and N. Camaioni, *Macromol. Chem. Phys.*, 2014, **215**, 452–457.
27 D. A. M. Egbe, B. Cornelia, J. Nowotny, W. Guenther and E. Klemm, *Macromolecules*, 2003, **36**, 5459–5469.
28 D. A. M. Egbe, H. Tillmann, E. Birckner and E. Klemm, *Macromol. Chem. Phys.*, 2001, **202**, 2712–2726.
29 M. Montalti, A. Credi, L. Prodi and T. Gandolfi, *Handbook of Photochemistry*, CRC Press, Taylor & Francic, Boca Raton, 2006, 3rd edn.
30 D. A. M. Egbe, C. Roll, E. Birckner, U. Grummt, R. Stockmann and E. Klemm, *Macromolecules*, 2002, **35**, 3825–3837.
31 P. Borsenberger and D. Weiss, in *Organic Photoreceptors for Xerography*, Marcel Dekker, New York, 1998.
32 N. Camaioni, F. Tinti, A. Esposti, S. Righi, Ö. Usluer, S. Boudiba and D. A. M. Egbe, *Appl. Phys. Lett.*, 2012, **101**, 053302.
33 H. Scher and E. Montroll, *Phys. Rev. B*, 1975, **12**, 2455–2477.
34 R. Kline and M. McGehee, *J. Macromol. Sci., Polym. Rev.*, 2006, **46**, 27–45.
35 Y. Olivier, D. Niedzialek, V. Lemaur, W. Pisula, K. Müllen, U. Koldemir, J. Reynolds, R. Lazzaroni, J. Cornil and D. Beljonne, *Adv. Mater.*, 2014, **26**, 2119–2136.
36 S. Rathgeber, J. Perlich, F. Kühnlenz, S. Türk, D. A. M. Egbe, H. Hoppe and R. Gehrke, *Polymer*, 2011, **52**, 3819–3826.
37 R. Noriega, J. Rivnay, K. Vandewal, F. P. V. Koch, N. Stingelin, P. Smith, M. F. Toney and A. Salleo, *Nat. Mater.*, 2013, **12**, 1038–1044.
38 P.-H. Chu, L. Zhang, N. S. Colella, B. Fu, J. O. Park, M. Srinivasarao, A. L. Briseño and E. Reichmanis, *ACS Appl. Mater. Interfaces*, 2015, **7**, 6652–6660.

 